J Mater Sci (2009) 44:170–178
DOI 10.1007/s10853-008-3112-1

Thermal stability and thermal degradation kinetics of poly(ethylene 2,6-naphthalate)/poly(trimethylene terephthalate) blends

Yingjin Wang · Haixian Ren · Wenya Liu · Mingtao Run · Hairong Zhang

Received: 27 March 2008 / Accepted: 10 November 2008 / Published online: 27 November 2008

Abstract The kinetics of thermal degradation of poly (ethylene 2,6-naphthalate)/poly(trimethylene terephthalate) (PEN/PTT) blends with different weight ratio were investigated by thermogravimetry analysis from ambient temperature to 800 °C in flowing nitrogen. The kinetic parameters, including the activation energy E_a, the reaction order n, and the pre-exponential factor ln(Z), of the degradation of the PEN/PTT blends were evaluated by three single heating rate methods and advanced isoconversional method developed by Vyazovkin. The three single heating rate methods used in this work include Friedman, Freeman–Carroll, and Chang method. The effects of the heating rate, the calculation methods, and the content of the PEN component on the thermal stability and degradation kinetic parameters of the PEN/PTT blends were systematically discussed. The PEN/PTT blends which degraded in two distinct stages were stable under nitrogen, also, the maximum rate of weight loss increased linearly with increasing of heating rate and decreased with increasing of PEN content. The obtained kinetics data suggested that the introduction of PEN component increased the activation energy, enhanced the stability of the blend system, and affected the process of degradation of PEN/PTT blend.

Y. Wang (✉) · H. Ren · H. Zhang
Lab of Biochemical Analysis, Xinzhou Teacher's University, Xinzhou 034000, China
e-mail: yingjinyaya@hotmail.com

W. Liu
China Vocational and Technical College, Shanghai 201404, China

M. Run
College of Chemistry & Environmental Science, Hebei University, Baoding 071002, China

Introduction

Poly(ethy1ene 2,6-naphthalate) (PEN), featuring a molecular structure of a naphthalene ring instead of the benzene ring in PET, is used as a high-performance polymer and that has superior strength, heat stability, and barrier properties due to its increased chain stiffness [1], thus PEN has been found in a variety of applications, such as tire cords of automobiles [2] and base films of videotapes, etc. Poly(trimethylene terephthalate) (PTT) was first patented by Whinfield and Dickson [3] in 1946 and commercially produced by Shell Chemicals until the 1990s. Many properties of PTT are between those of poly(ethylene terephthalate) (PET) and poly(butylene terephthalate) (PBT), such as crystallization rate and glass transition temperature. Moreover, it combines the two key advantages of PET and PBT into one polymer and it has an important application in the textile industry [4] and as a promising engineering thermoplastic [5].

Polymer blending is an ideal alternative for producing new polymeric materials with desirable properties, which does not have to synthesize a totally new material. Other advantages for polymer blending are versatility, simplicity, and inexpensiveness. Due to the similarity in the chemical structure of these linear aromatic polyesters, numerous research works related to various aspects of polyesters' blends are available in the reported literatures. Blends of polyesters were investigated widely, such as PEN and poly(butylene 2,6-naphthalate) (PBN) [6], PET/PBT [7], PET/PEN [8], PTT/PET [9], PTT/PBT [10]. For PTT/PEN

blend, Supaphol and coworkers [11] studied the miscibility, melting, and crystallization behavior of PTT/PEN blends. PTT and PEN are miscible in the amorphous state in all of the blends compositions, as evidenced by a single, composition dependent glass transition temperature (T_g) observed for each blend composition. The variation in the T_g value with the blend composition is well predicted by the Gordon–Taylor equation, with the fitting parameter being 0.57. Run et al. [12, 13] investigated the isothermal, nonisothermal crystallization kinetics, and the crystal morphology characters of the PTT/PEN blends. Avrami analysis of the isothermal-crystallization process of PTT/PEN showed primary and second stages. In the primary stage, n is in the range of 3.0–3.3, the crystal nucleation type include both thermal and athermal nucleation, and the growth dimension should predominantly be three-dimensional. However, so far, to the best of our knowledge, there are few reports on the kinetics of the thermal degradation of PEN/PTT blends.

Thermal stability of a polymeric material is one of the most important properties for both processing and application. Thermogravimetry (TG) is the most widely used technique to characterize thermal decomposition of polymer materials. In this article, thermogravimetry (TG) and derivative thermogravimetry (DTG) measurements of PEN/PTT blends are reported; the thermal degradation kinetics of PEN/PTT blends with the weight ratio, PEN/PTT(80/20) and (20/80), were studied by several kinds of calculation methods through nonisothermal TG thermograms, such as Friedman, Chang, Freeman–Carroll, and the advanced isoconversional methods. The dependency of the kinetics parameters on the heating rate and calculation method were discussed in detail.

Experiment

Materials

The PEN homopolymer was supplied in pellet form by Honeywell (USA) with an intrinsic viscosity of 0.89 dL/g measured in phenol/tetrachloroethane solution (60/40, w/w) at 30 °C. The PTT homopolymer was supplied in pellet form by Shell Chemicals (USA) with an intrinsic viscosity of 0.92 dL/g measured in a phenol/tetrachloroethane solution (50/50, w/w) at 25 °C.

Blends preparation

The materials were dried in a vacuum oven at 140 °C for 12 h before preparing blends. The dried pellet of PTT and PEN were mixed together with different weight ratio of PEN/PTT as following: B1: 100/0; B2: 80/20; B3: 60/40; B4: 40/60; B5: 20/80; B6: 0/100, and then melt-blended in a ZSK-25WLE WP self-wiping, co-rotating twin-screw extruder, operating at a screw speed of 60 rpm and at a die temperature of 300 °C. The resultant blend ribbons were cooled in cold water, cut up, re-dried before being used in TGA.

Thermogravimetry analysis (TGA)

TG and DTG curves were gained by using a Perkin-Elmer 7 series analyzer under a dynamic nitrogen atmosphere flowing 50 mL/min, varying heating rate from 5 to 40 °C/min, while the weight of sample in a form of pellet was kept at 10.0 ± 0.1 mg.

Theoretical consideration

There are several methods (proposed by Friedman [14], Freeman and Carroll [15], Chang [16], Kissinger [17], Flynn–Wall [18], Horrowitz and Metzger [19], Coats and Redern [20], Van Krevelen et al. [21], Ozawa [22], Vyazovkin [23, 24]) for calculating kinetic parameters which depend not only on the experimental conditions but also on the mathematical treatment of the data. In this article, the Friedman, Freeman and Carroll, and Chang methods are employed to evaluate the activation energy E_a, reaction order n, and frequency factor $\ln(Z)$ based on a single heating rate measurement without making any assumptions. The descriptions of the three methods are not given in detail because the methods for evaluating the kinetic parameters from TG and DTG traces are easily available from the literatures [14–16]. The equations employed in the methods are listed below.

Friedman method

$$\ln(\mathrm{d}a/\mathrm{d}t) = \ln(Z) + n\ln(1-a) - E_a/RT \quad (1)$$

where a is the weight loss of the sample undergoing degradation at time t, R is the gas constant, and T is the absolute temperature. The plot of $\ln(\mathrm{d}a/\mathrm{d}t)$ as a function of $1/T$ should be linear with a slope equal to $-E_a/R$. Additionally, the $E_a/(nR)$ value could be determined from the slope of a linear plot of $\ln(1-a)$ versus $1/T$.

Chang method

Equation 1 can be rewritten in the following form:

$$\ln[(\mathrm{d}a/\mathrm{d}t)/(1-a)^n] = \ln(Z) - E_a/RT \quad (2)$$

a plot of $\ln[(\mathrm{d}a/\mathrm{d}t)/(1-a)^n]$ against $1/T$ will yield a straight line if the decomposition order n is collected correctly. The $-E_a/R$ and $\ln(Z)$ values are calculated by the slope and intercept of this line.

Freeman–Carroll method

$$\Delta\ln(\mathrm{d}a/\mathrm{d}t)/\Delta\ln(1-a) = n - (E_a/R)\Delta(1/T)/\Delta\ln(1-a) \quad (3)$$

the $\Delta\ln(\mathrm{d}a/\mathrm{d}t)$ and $\Delta\ln(1-a)$ values are taken at regular intervals of $1/T$, in this case $\Delta(1/T) = 0.00002\ \mathrm{K}^{-1}$. By plotting $\Delta\ln(\mathrm{d}a/\mathrm{d}t)/\Delta\ln(1-a)$ against $\Delta(1/T)/\Delta\ln(1-a)$, a straight line was obtained, and the slope and intercept are equal to $-E_a/R$ and n, respectively. In addition, the $\ln(Z)$ values can be evaluated using Eq. 1.

The advanced isoconversional method

The advanced isoconversional method developed by Vyazovkin is employed to describe the process of degradation. According to this method, for a set of n experiments carried out at different heating programs, the activation energy is determined at any particular value of a by finding the value of E_a that minimizes the function.

$$\Phi(E_a) = \sum_{i=1}^{n}\sum_{j\neq i}^{n}\frac{J[E_a, T_i(t_a)]}{J[E_a, T_j(t_a)]} \quad (4)$$

where

$$J[E_a, T_i(t_a)] \equiv \int_{t_{a-\Delta a}}^{t_a} \exp\left[\frac{-E_a}{RT_i(t)}\right]\mathrm{d}t \quad (5)$$

where the subscript a is the value related to a given extent of conversion and a is varied from Δa to $1 - \Delta a$ with a step $\Delta a = \mathrm{m}^{-1}$, where m is the number of intervals chosen for analysis. The integral J in Eq. 5 is evaluated numerically by using the trapezoid rule. The minimization procedure is repeated for each value of a to find the dependence of E_a on a.

Results and discussion

Thermal stability behavior of PEN/PTT blends

TG is widely used for evaluating the thermal stability of polymers because only a small amount of sample is needed and the entire study will be completed within a few hours. The TG curves of six kinds of PEN/PTT blends under nitrogen are shown in Fig. 1. All the six samples are stable up to approximately 360 °C, which suggests that all the six samples have excellent thermal stability. All the six samples exhibit two weight loss stages, which maybe attributed to the existence of two kinds of phase states in blend system. With increasing PEN content, the TG curves gradually shift to higher temperature, which indicates that the stability of PEN/PTT samples is enhanced by PEN

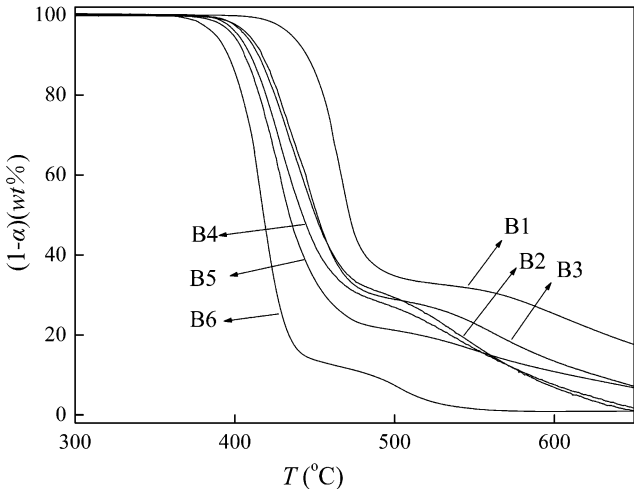

Fig. 1 TG curves of various PEN/PTT blends in dynamic nitrogen at the heating rate of 20 °C/min

Table 1 Parameters of the TG curves for various PEN/PTT blends

Samples	T_{on} (°C)	T_{md} (°C)	T_d 5% loss (°C)	T_d 10% loss (°C)
B1	401.1	460.9	435.5	445.0
B2	383.3	447.3	408.8	417.1
B3	380.6	434.5	406.5	414.8
B4	377.2	427.8	402.0	409.8
B5	372.4	426.8	399.1	405.9
B6	362.8	415.3	388.1	396.0

component. The parameters of the TG curves for various PEN/PTT blends are listed in Table 1. The results show that the sequence of onset temperature (T_{on}), peak temperature (T_{dm}) of DTG, and decomposition temperature of 5% and 10% weight loss of the blends are as follow B1 > B2 > B3 > B4 > B5 > B6. These results suggest that the thermal stability of PEN/PTT blends is: B1 > B2 > B3 > B4 > B5 > B6, which maybe ascribed to the difficult decomposition of PEN component with higher melting temperature ($T_m = 264.0$ °C) and easy decomposition of PTT component with lower melting temperature ($T_m = 227.1$ °C).

The nonisothermal degradation behavior of B2 and B5 blends

The TG and DTG curves of B2 and B5 blends in nitrogen at heating rate of 5, 10, 20, 30, 40 °C/min are shown in Figs. 2 and 3, respectively. The kinetics parameters are listed in Table 2. Obviously, the TG and DTG curves of both B2 and B5 blends show that two weight loss stages occur during degradation. Generally speaking, the higher

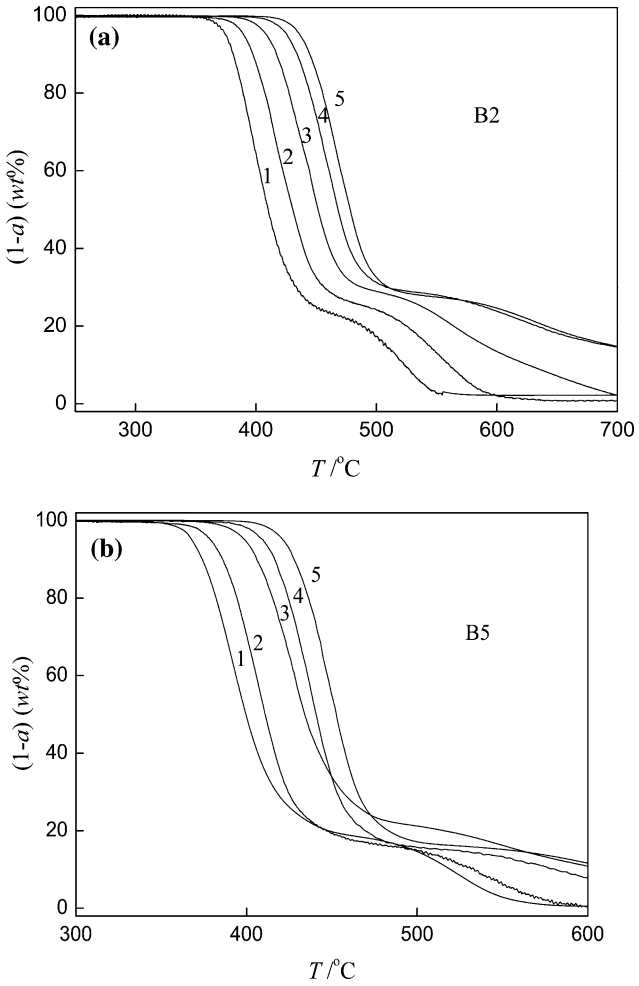

Fig. 2 Dynamic TG curves for sample B2 (**a**) and B5 (**b**) at five heating rates (1–5 °C/min, 2–10 °C/min, 3–20 °C/min, 4–30 °C/min, 5–40 °C/min)

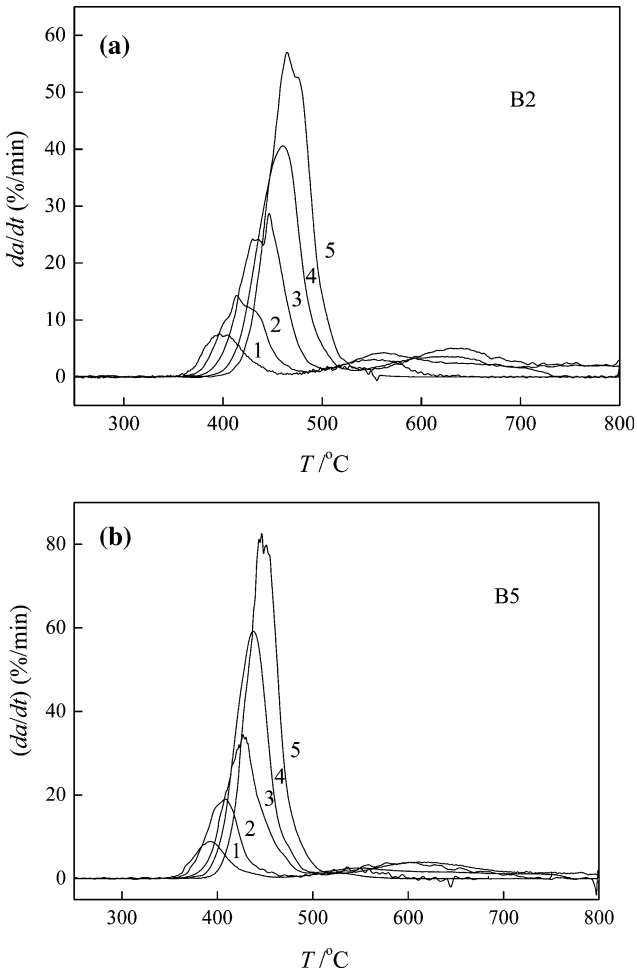

Fig. 3 Dynamic DTG curves for sample B2 (**a**) and B5 (**b**) at five heating rates (1–5 °C/min, 2–10 °C/min, 3–20 °C/min, 4–30 °C/min, 5–40 °C/min)

the heating rate, the later is the degradation. As it is expected the T_{on} values increase from 355.4 °C to 408.2 °C, the T_{dm} values increase from 397.7 °C to 464.5 °C for B2 blends, and T_{on} from 343.7 °C to 400.3 °C, T_{dm} from 392.7 °C to 446.4 °C for B5 blends as the heating rate increases from 5 to 40 °C/min, which is attributed to the low time scale that allows the polymer to degrade with increasing heating rate, thus requiring a higher temperature to initiate degradation. Comparing B2 with B5, it is easy to find that both the T_{on} and T_{dm} values of B2 at various heating rates are lager than that of B5, which signify that the stability of the PEN/PTT blends is enhanced by the PEN component. Furthermore, the loss weight of first degradation end of B2 blends listed in Table 2 are higher than that of B5 at a given heating rate, which also confirm that the samples with more PEN component has a higher thermal stability than that with less one.

Kinetics of nonisothermal decomposition of PEN/PTT blends analyzed by single heating rate methods

Friedman method

All of the methods, Friedman, Chang, and Freeman–Carroll can determine the kinetic parameters for the thermal degradation of PEN/PTT blends by using only one heating rate. According to Friedman's theory and plots of $\ln(1-a)$ versus $1/T$ and $\ln(da/dt)$ versus $1/T$ at a given heating rate, a series of straight lines are obtained if Friedman analysis is valid, and the degradation kinetic parameters n and $-E_a/R$ can be derived from the slope. The results of Friedman analysis for both B2 and B5 blends are shown in Fig. 4a and b, respectively. Also, the kinetics parameters of the first thermal degradation stage are listed in Table 3. Because the line of either $\ln(1-a)$ versus $1/T$ or $\ln(da/dt)$ versus $1/T$ overlapped each other, the Waterfall Graph (in Microcal

Table 2 Parameters of TG and DTG curves for sample B2 and B5

Heating rate β (°C/min)	B2				B5			
	T_{on} (°C)	T_{dm} (°C)	wt^{a}_{end} (%)	$wt_{(T=600\ °C)}$ (%)	T_{on} (°C)	T_{dm} (°C)	wt^{a}_{end} (%)	$wt_{(T=600\ °C)}$ (%)
5	355.4	397.7	22.54	2.3	343.7	392.7	17.31	0.4
10	360.5	413.7	25.39	2.2	357.5	408.1	17.20	0.5
20	383.3	446.4	28.70	13.5	374.3	426.2	21.19	7.9
30	396.2	460.3	28.61	23.8	386.2	437.3	16.12	10.8
40	408.2	464.5	28.76	24.6	400.3	446.4	16.40	11.7

[a] The loss weight of first degradation end

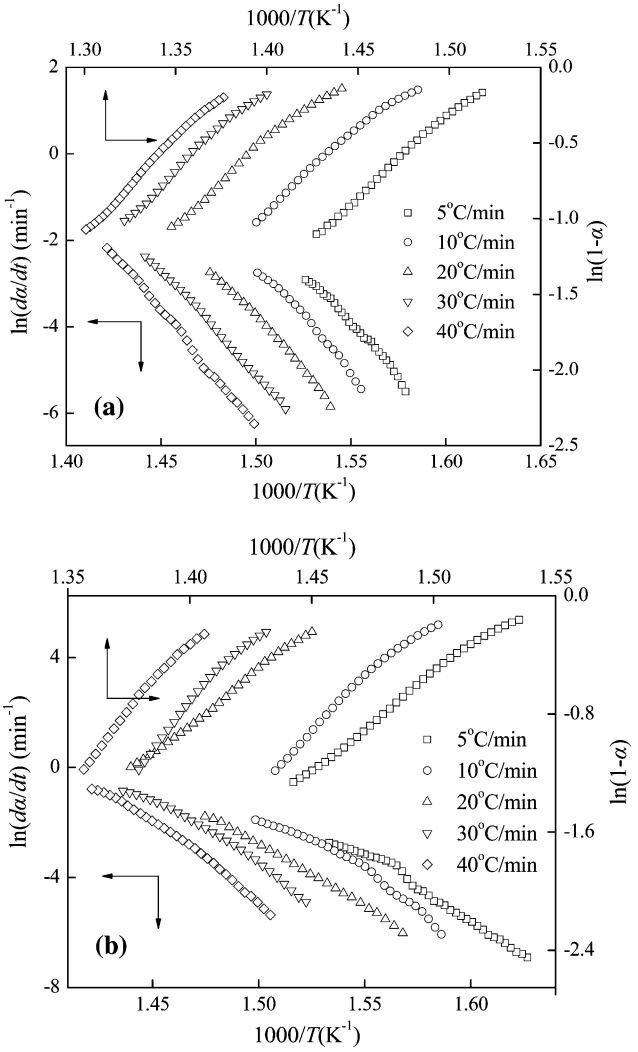

Fig. 4 Friedman plots of $\ln(1-a)$ or $\ln(\mathrm{d}a/\mathrm{d}t)$ versus $1/T$ for sample B2 (**a**) and B5 (**b**) at five heating rates

Origin 7.0, Microcal Software) is used to obtain a distinct view. Each dataset is displayed as a line data plot, which is offset by a specified amount in both the X and Y direction. For Friedman method, the absolute X and Y values do not affect the calculation of thermal degradation kinetic parameters, so offset X- and Y-axes are omitted here.

Table 3 Kinetic parameters of thermal degradation of B2 and B5 blend under nitrogen calculated by Friedman method

β (°C/min)	B2			B5		
	n	E_a (kJ/min)	$\ln(Z)$ (min^{-1})	n	E_a (kJ/min)	$\ln(Z)$ (min^{-1})
5	1.9	167.3	30.7	1.7	164.9	32.8
10	2.1	175.9	29.7	1.3	157.1	32.3
20	2.0	167.4	28.7	1.5	156.1	27.9
30	1.8	170.1	28.1	1.1	162.2	30.4
40	1.9	186.8	30.4	1.2	185.0	33.9
Average	1.9	173.5	29.5	1.3	165.0	31.4

Chang method

Figure 5 shows the relationship proposed by Chang method where the degradation orders are assumed to be from 1.5 to 1.9 for B2 and from 1.1 to 3.4 for B5 blends. The Waterfall Graph was also used for the Chang plots. For the Chang method, the absolute X and Y also do not affect the calculation of thermal degradation kinetic parameters, so the offset X and Y are also omitted here. The degradation kinetics parameters obtained by the Chang method are summarized in Table 4.

Freeman–Carroll method

The method developed by Freeman and Carroll is also employed to describe the nonisothermal degradation process. At a given heating rate, the plot of $\Delta\ln(\mathrm{d}a/\mathrm{d}t)/\Delta\ln(1-a)$ against $\Delta(1/T)/\Delta\ln(1-a)$ will give a straight line with an intercept of n and a slope of $-E_a/R$. Figure 6 shows the relationship of $\Delta\ln(\mathrm{d}a/\mathrm{d}t)/\Delta\ln(1-a)$ against $\Delta(1/T)/\Delta\ln(1-a)$of both B2 and B5, where the value of $\Delta(1/T)$ equals 0.00002 K^{-1}, and the values of n, E_a, and $\ln(Z)$ are listed in Table 5. Because the Freeman–Carroll

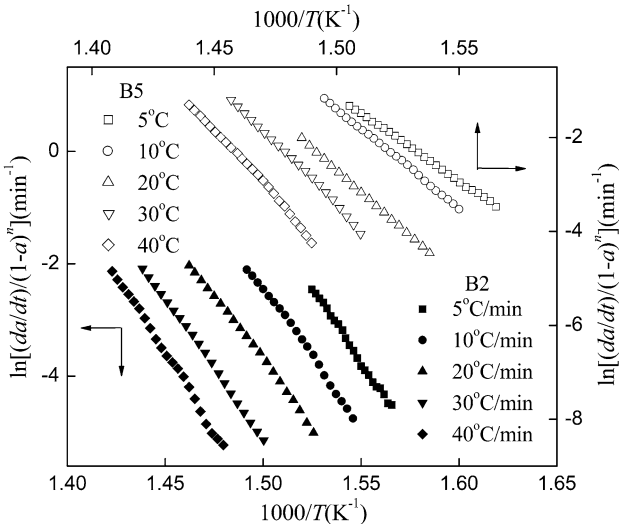

Fig. 5 Chang plots of $\ln[(\mathrm{d}a/\mathrm{d}t)/(1-a)^n]$ against $1/T$ for thermal degradation of B2 and B5 in nitrogen at five heating rates

Table 4 Kinetic parameters of thermal degradation of B2 and B5 blend under nitrogen calculated by Chang method

β (°C/min)	B2			B5		
	n	E_a (kJ/min)	ln(Z) (min^{-1})	n	E_a (kJ/min)	ln(Z) (min^{-1})
5	1.5	192.8	32.6	1.1	129.7	28.6
10	1.6	177.2	30.4	1.2	152.9	31.3
20	1.7	165.7	27.0	1.3	168.6	29.7
30	1.8	179.5	28.4	1.3	189.1	33.5
40	1.9	201.3	32.3	1.4	207.9	35.9
Average	1.7	183.3	30.1	1.3	169.6	31.9

lines also overlapped each other, we plot these lines on a parallel plane.

The effect of calculation method

From Figs. 4, 5, and 6 and Tables 3, 4, and 5, it is obvious that the parameters depend not only on the experimental conditions, but also on the mathematical treatment of the data. The results obtained by the Friedman, Chang, and Freeman–Carroll method are in agreement with one another, except that the n values gained from Friedman method are little higher. The results derived from Freeman–Carroll and Chang methods have no signification distinction.

The reason why the Friedman, Freeman–Carroll, and Chang method do not give the same results is that different calculation method, respectively, appropriate in different temperature ranges. Although we assume that the temperature range does not vary in every mathematical method,

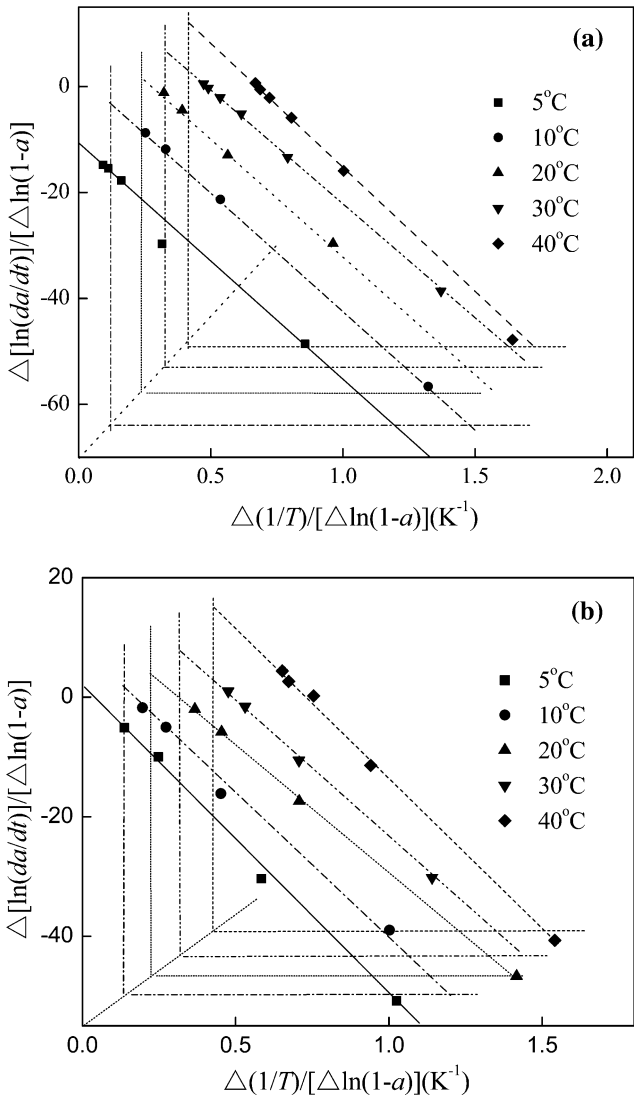

Fig. 6 Freeman–Carroll plots of $\Delta\ln(\mathrm{d}a/\mathrm{d}t)/\Delta\ln(1-a)$ against $\Delta(1/T)/\Delta\ln(1-a)$ for degradation of B2 (**a**) and B5 (**b**) in nitrogen at five heating rates

Table 5 Kinetic parameters of thermal degradation of B2 and B5 blend under nitrogen calculated by Freeman–Carroll method

β (°C/min)	B2			B5		
	n	E_a (kJ/min)	ln(Z) (min^{-1})	n	E_a (kJ/min)	ln(Z) (min^{-1})
5	1.5	173.5	31.3	0.9	171.5	33.1
10	1.4	175.2	32.1	0.9	158.0	32.3
20	1.5	172.8	31.7	1.2	154.7	29.6
30	1.7	180.7	28.4	1.3	179.1	33.1
40	1.7	190.2	33.3	1.4	190.0	36.5
Average	1.6	178.5	31.4	1.1	170.6	32.9

the kinetic parameters change more or less with them. In the case of Friedman method (see Fig. 4 and Table 3), the E_a values derived from the slope of ln(da/dt) versus $1/T$.

The linear relation between ln(da/dt) versus 1/T for B2 and B5 sample stands only in the temperature range from T_{dm} −56 °C to T_{dm} −33 °C and T_{dm} −54 °C to T_{dm} −21 °C (where the T_{dm}-A is a average values at five heating rate), respectively. Then from the slope of ln(1 − a) versus 1/T and the derived E_a value, the n value can be calculated. However, the relationship between ln(1 − a) versus 1/T for B2 and B5 samples remains linear in the temperature range from T_{dm} −16 °C to T_{dm} +28 °C and T_{dm} −12 °C to T_{dm} + 20 °C. Finally, ln(Z) can be determined by substituting E_a and n into Eq. 1. Comparing with E_a/RT, both ln(da/dt) and ln(1 − a) are so small that ln(Z) is mainly determined by E_a value. Therefore, the E_a and ln(Z) values for B2 and B5 samples derived from Friedman method mainly indicate the thermal degradation behavior in the temperature range from T_{dm} −56 °C to T_{dm} −33 °C and T_{dm} −54 °C to T_{dm} −21 °C. On the contrary, in the case of Chang method (see Fig. 6 and Table 5), the linear relation can be gained in the temperature range from T_{dm} −59 °C to T_{dm} −21 °C for B2 and from T_{dm} −50 °C to T_{dm} −18 °C for B5. In the case of Freeman–Carroll method (see Fig. 5 and Table 4), the linear relation can be gained in the temperature range from T_{dm} −56 °C to T_{dm} −20 °C for B2 and from T_{dm} −52 °C to T_{dm} −23 °C for B5. Moreover, according to Eq. 1 and Freeman–Carroll plots, the E_a, n, ln(Z) can be gained. Meanwhile, the E_a and ln(Z) values can be derived directly by Chang method.

From the above analysis, it can be concluded that the Freeman–Carroll have similar temperature ranges with Chang methods, both of them are wider than that of Friedman method. Consequently, the Freeman–Carroll and Chang methods provide very similar values of kinetic parameters. Generally speaking, for a thermal degradation process, a wider temperature range will result in better reliability with smaller errors [25]. Although the Chang method has the widest temperature range, one cannot use the method alone because the n value must be assumed before calculation. Moreover, the Chang method has low sensitivity to n values, which means that a good linear relation can be obtained in a wide range of n values. Therefore, Freeman–Carroll is the most reliable method, whereas the Chang method can be used to check the results gained by other methods. Furthermore, for the Friedman method, the temperature range is wide enough to obtain credible results.

The effect of the heating rate

From Tables 2, 3, 4, and 5, it is can be concluded that the kinetic parameters of B2 and B5 samples change with varying the heating rate, the T_{on}, T_{dm}, ln(Z) values increase significantly, whereas the n values stay roughly the same as the heating rate changes from 5 to 40 °C/min. That is to say, when the heating rate is higher enough, the effect of the concentration of decomposition products from B2 and B5 sample on thermal degradation reaction will remain roughly unchanged [26].

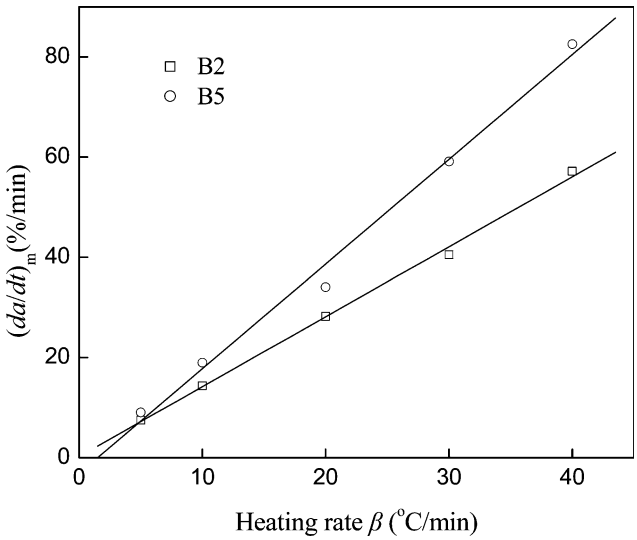

Fig. 7 Effects of heating rate on the maximum decomposition rate of the first decomposition stage of B2 and B5 samples

Figure 7 shows the good linear dependency between (da/dt)$_m$ at the first decomposition stage and heating rates for all degradation process of B2 and B5 studied in this article, and the (da/dt)$_m$ values increase linearly with increasing heating rates. The variation of these kinetic parameters reveals the change of thermal degradation mechanism, i.e., the transformation from the diffusion kinetics into the decomposition-controlled kinetics, or vice versa [26]. As the cooling rate increased, the degradation of the materials occurred rather inhomogeneously (i.e., from outside in), due to the low thermal diffusivity of the polymeric materials. This probably caused the materials to form a degraded skin layer. As the degradation progressed, the diffusion of the degraded substances changed. Consequently, higher kinetic parameters were observed with increasing heating rate.

Kinetics of nonisothermal decomposition of PEN/PTT blends analyzed by the advanced isoconversional method

The advanced isoconversional method has been widely applied in the degradation of polymer and other materials because the method can offer two major advantages over the frequently used multiple heating rate methods of Flynn–Wall and Ozawa. The first advantage is that the method has been designed to treat the kinetics that occur under an arbitrary variation in temperature, $T(t)$, which allows one to account for self-heating/cooling detectable

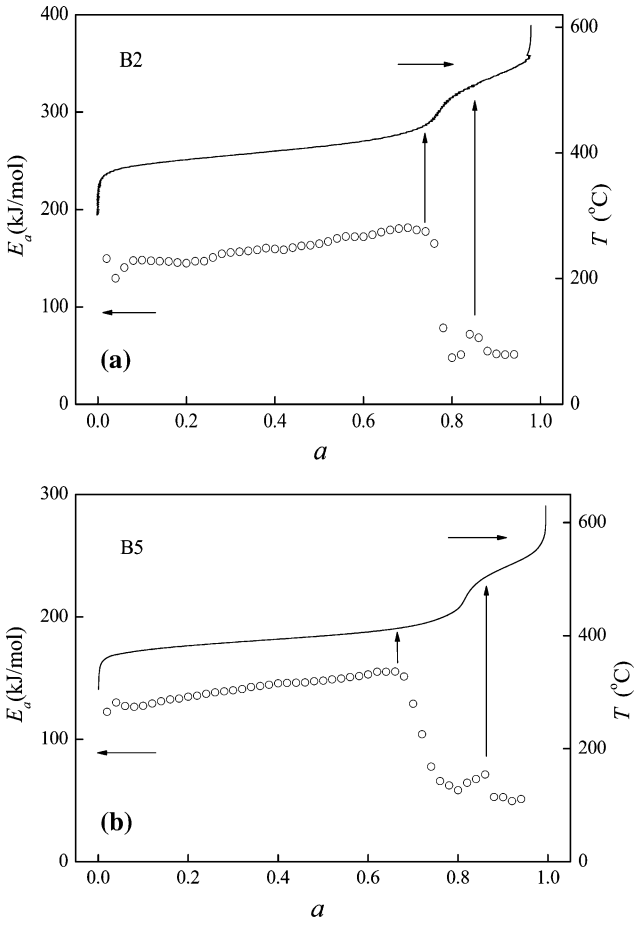

Fig. 8 TGA curve for decomposition of B2 and B5 at heating rate of 5 °C/min (upper trace) compared to the dependence of the activation energy on the extent of decomposition conversion (lower trace)

by the thermal sensor of the instrument. The second advantage is associated with performing the integration over small time segments, which allows the elimination of a systematic error [24] occurring in the Flynn–Wall and Ozawa methods when E_a varies significantly with a.

Figure 8 displays the results of the isoconversional kinetic analysis for the thermal degradation of B2 and B5 blend in the atmosphere of nitrogen. Both B2 and B5 blends exhibit two decomposition steps. For B2 blend, the major decomposition step ($a < 0.76$) shows a rise in activation energy from 129.4 to 181.2 kJ/mol. The slow second step ($a > 0.8$) starts with an abrupt drop in the activation energy and the average activation energy for this step is about 58.4 kJ/mol. For B5 blend, the activation energy increases from 122.2 to 156.5 kJ/mol at the major decomposition ($a < 0.67$), and the activation energy at the second step ($a > 0.74$) is about 44.8 kJ/mol. The whole process of B2 degradation demonstrates evidently larger activation energy as compared with that of B5 degradation, which suggests that B2 is more stable than B5 blend. In other words, PEN component improves the stability of the PEN/PTT blend. This phenomenon maybe attributed to the difference in content of naphthalene structure unit in the PEN/PTT blend. It is well known that the higher the content of the aromatic carbon atoms, better is the thermal stability.

Figure 8 compares the E_a dependence against the experimentally observed mass loss curve for B2 (a) and B5 (b) blends. The two decomposition steps are associated with variations in the E_a dependence. The E_a dependence determined for the first and major step of the B2 and B5 decomposition suggests that this step maybe involved in two decomposition pathways. With increasing the temperature, the pathway having smaller activation energy is taken over by the pathway that has greater activation energy. The slow rate and low activation energy for the second decomposition step suggest that further decomposition may be limited by diffusion [27].

Thermal stability

No matter which method was used above, the fundamental equation is the same:

$$da/dt = Z(1-a)^n \exp(-E_a/RT) \quad (6)$$

because the value of $(1 - a)$ is always less or equal to 1, da/dt decreases with increasing n, and the zero order ($n = 0$) characterizes the most rapid degradation reaction [26]. From Eq. 6, it can be concluded that higher n and E_a or a lower Z value results in a lower da/dt value, which means higher thermal stability.

As shown in Tables 3, 4, and 5, the average n, T_{on}, and T_{dm} values calculated from the heating rate for B2 are larger than those for B5, meanwhile, the da/dt and $\ln(Z)$ at different heating rates for B2 are lower than those for B5. This may attribute to the different molecular structures between PEN and PTT. It has been previously mentioned that the higher the n, the slower is the degradation rate. More aromatic carbon atoms (or less hydrogen atom) will decrease the thermal degradation rate and increase the thermal stability [28]. The B2 blend exhibits a higher n value and lower degradation rate da/dt than B5 because of the higher content of PEN component in B2 blends which possesses more stable naphthalene units than PTT component.

Conclusions

All the six PEN/PTT blends show two weight-loss stages during degradation process in nitrogen .The parameters, such as activation energy E_a, degradation order n, and frequency factor $\ln(Z)$, calculated by the Friedman, Chang,

Freeman–Carroll and the advanced isoconversional methods suggest that PEN/PTT blend exhibits good thermal stability, and the thermal stability of the sample is improved with increase of PEN content.

In the case of single heating rate methods, Freeman–Carroll method can provide the most reliable E_a, n, and $\ln(Z)$ values, the Friedman method may offer a little lower values, and the Chang method can only be used to validate the outcomes from other methods. Additionally, the results derived from the advanced isoconversional method exhibit an excellent dependence on PEN/PTT blend mass loss trace and these results are much less than those given by single heating rate method.

Acknowledgement This work was funded by Grant (B2007000148) from Natural Science Foundation of Hebei province.

References

1. Nakamae K, Nishino T, Tada K, Kannamoto T, Ito M (1993) Polymer 34:3322
2. Van den Heuvel CJM, Klop EA (2000) Polymer 41:4249
3. Whinfield JR, Dickson JT (1946) British Patent 578,079, 14 June 1946
4. Wu J, Schultz JM, Samon JM, Pangelinan AB (2001) Polymer 42:7141
5. Grande JA (1997) Mod Plast 12:97
6. Yoon KH, Lee SC, Park OO (1995) Polym Eng Sci 35:1807
7. Yu Y, Choi KJ (1997) Polym Eng Sci 37:91
8. Supaphol P, Dangseeyun N, Thanomkiat P, Nithitanakul M (2004) J Polym Sci Polym Phys 42:676
9. Dangseeyun N, Supaphol P, Nithitanakul M (2004) Polym Test 23:187
10. Rwei SP (1999) Polym Eng Sci 39:2475
11. Krutphun P, Supaphol P (2005) Eur Polym J 41:1561
12. Run M, Wang Y, Yao C, Gao J (2006) Thermochim Acta 447:13
13. Run M, Wang Y, Yao C, Zhao H (2006) J Appl Polym Sci 103:3316
14. Friedman HL (1964) J Polym Sci Part C 6:183
15. Freeman ES, Carroll BJ (1958) J Phys Chem 62:394
16. Chang WL (1994) J Appl Polym Sci 53:1759
17. Kissinger HE (1957) Anal Chem 29:1702
18. Flynn JH, Wall LA (1966) J Polym Sci Part B 4:323
19. Horowitz HH, Metzger G (1963) Anal Chem 35:1464
20. Coat AW, Redern JP (1964) Nature 201:68
21. Van Krevelen DW, Van Heerden C, Huntjens FJ (1951) Fuel 30:253
22. Ozawa T (1965) Bull Chem Soc Jpn 38:1881
23. Vyazovkin S (1997) J Comput Chem 18:393
24. Vyazovkin S (2001) J Comput Chem 22:178
25. Wang X, Li X, Yan D (2000) J Appl Polym Sci 78:2025
26. Li Z, Ma J, Zhu X, Liang B (2004) J Appl Polym Sci 91:3915
27. Vyazovkin S (1996) Int J Chem Kinet 28:95
28. Tang W, Li X, Yan D (2004) J Appl Polym Sci 91:445